HHS Public Access

Author manuscript

Cell Rep. Author manuscript; available in PMC 2017 February 16.

Published in final edited form as:

Cell Rep. 2017 February 07; 18(6): 1543–1557. doi:10.1016/j.celrep.2017.01.031.

ATXN1L, CIC, and ETS Transcription Factors Modulate Sensitivity to MAPK Pathway Inhibition

Belinda Wang[1,2,3,6], **Elsa Beyer Krall**[1,2,3,6], **Andrew James Aguirre**[1,2,3,6], **Miju Kim**[1,2,3], **Hans Ragnar Widlund**[4], **Mihir Bhavik Doshi**[1,2,3], **Ewa Sicinska**[1,5], **Rita Sulahian**[1,2,3], **Amy Goodale**[2], **Glenn Spencer Cowley**[2], **Federica Piccioni**[2], **John Gerard Doench**[2], **David Edward Root**[2], and **William Chun Hahn**[1,2,3,*]

[1]Department of Medical Oncology, Dana-Farber Cancer Institute, Boston, MA 02215, USA

[2]Broad Institute of Harvard and MIT, Cambridge, MA 02142, USA

[3]Department of Medicine, Brigham and Women's Hospital and Harvard Medical School, Boston, MA 02115, USA

[4]Department of Dermatology, Brigham and Women's Hospital, Boston, MA 02115, USA

[5]Center for Molecular Oncologic Pathology, Brigham and Women's Hospital and Dana-Farber Cancer Institute, Boston, MA 02115, USA

SUMMARY

Intrinsic resistance and RTK-RAS-MAPK pathway reactivation has limited the effectiveness of MEK and RAF inhibitors (MAPKi) in *RAS*- and *RAF*-mutant cancers. To identify genes that modulate sensitivity to MAPKi, we performed genome scale CRISPR-Cas9 loss-of-function screens in two *KRAS*-mutant pancreatic cancer cell lines treated with the MEK1/2 inhibitor trametinib. Loss of CIC, a transcriptional repressor of ETV1, 4, and 5, promoted survival in the setting of MAPKi in cancer cells derived from several lineages. *ATXN1L* deletion, which reduces CIC protein, or ectopic expression of ETV1, 4, or 5 also modulated sensitivity to trametinib. *ATXN1L* expression inversely correlates with response to MAPKi inhibition in clinical studies. These observations identify the ATXN1L-CIC-ETS transcription factor axis as a mediator of resistance to MAPKi.

*Lead Contact: william_hahn@dfci.harvard.edu (W.C.H.).

[6]Co-first author

SUPPLEMENTAL INFORMATION

Supplemental information includes Extended Experimental Procedures, seven figures, and three tables.

AUTHOR CONTRIBUTIONS

B.W., A.J.A., E.B.K., G.C., F.P., J.G.D., and W.C.H. designed the screens, and B.W., A.J.A., A.G., R.S., G.C., and F.P. performed the screens. B.W., A.J.A., E.B.K., G.C. and J.G.D. analyzed screen results. B.W., E.B.K., A.J.A., J.G.D. and W.C.H. designed *in vitro* experiments. E.B.K., B.W., M.K., M.B.D., and S.R. performed *in vitro* experiments. A.J.A. and E.S. designed *in vivo* experiments. E.S., A.J.A., and M.B.D. performed *in vivo* experiments. H.R.W. analyzed melanoma outcome data. B.W., E.B.K. and W.C.H. wrote the manuscript, and all authors edited the manuscript.

ACCESSION NUMBERS

RNA sequencing data can be found in the NCBI Gene Expression Omnibus (GEO: GSE78519).

INTRODUCTION

The *RAS* family (*KRAS, NRAS,* and *HRAS*) is frequently mutated in human cancers. Although the majority of cancers with mutant *RAS* depend on oncogenic RAS signaling for proliferation and survival, direct inhibitors of oncogenic RAS proteins have not yet been developed for clinical use (Chien et al., 2006; Cox et al., 2014; Stephen et al., 2014). An alternative approach to target *RAS*-mutant cancers is to inhibit downstream effector pathways. The RAF-MEK-ERK (MAPK) pathway is an important downstream effector of oncogenic *RAS* (Blasco et al., 2011; Collisson et al., 2012). Early clinical trials suggest that a subset of *KRAS*- or *BRAF*-mutant cancers respond to small molecule inhibitors of MEK or BRAF, though both intrinsic and acquired resistance limit therapeutic efficacy (Blumenschein et al., 2015; Chapman et al., 2011; Hyman et al., 2015; Infante et al., 2012).

Preclinical and clinical studies have shown that a major mode of intrinsic and acquired resistance to MEK or BRAF inhibitor monotherapy in *RAS*- or *BRAF*-mutant cancers is the reactivation of the RTK-RAS-MAPK pathway by mechanisms (Caunt et al., 2015; Lito et al., 2013), such as loss of feedback inhibition (Corcoran et al., 2012; Duncan et al., 2012); upregulated RTK signaling (Nazarian et al., 2010; Villanueva et al., 2010); *NF1* inactivation (Whittaker et al., 2013); or increased NRAS (Nazarian et al., 2010), A/B/C-RAF (Hatzivassiliou et al., 2010; Heidorn et al., 2010; Poulikakos et al., 2011; Thakur et al., 2013; Villanueva et al., 2010), COT (Johannessen et al., 2010), or MEK1/2 activity (Nikolaev et al., 2011; Wagle et al., 2011). These observations highlight a key role for sustained RTK/MAPK signaling in mediating resistance to pharmacologic inhibition of this pathway in *RAS*- or *BRAF*-mutant cancers.

Here we performed unbiased genome scale genetic screens to identify genes whose deletion promote survival in the context of MEK inhibition in K*RAS*-mutant pancreatic cancer cell lines. We extended our findings to *RAS*- and *RAF*-mutant cell lines of various lineages, and characterized the mechanistic basis of resistance to MAPK pathway inhibition (MAPKi).

RESULTS

Identification of Genes that Modulate Sensitivity to MEK Inhibition in *KRAS*-mutant Pancreatic Cancer Cell Lines

To identify genes whose deletion promote proliferation/survival in the context of MAPKi, we performed genome scale CRISPR-Cas9 knockout screens in 2 *KRAS*-mutant pancreatic cancer cells (PATU8902 and PATU8988T) treated with 2 different doses of the allosteric MEK1/2 inhibitor trametinib (Figure 1A). We screened PATU8902 cells with 100 nM trametinib (high dose), which robustly inhibits ERK phosphorylation and induces proliferative arrest or cell death (Figures S1A–B). For PATU8988T, we performed the screen using 10 nM trametinib (moderate dose), which modestly suppresses ERK phosphorylation and decreases cell proliferation by ~50% (Figures S1C–D). We used these different doses of trametinib to increase the dynamic range of the screens and used different genome scale sgRNA libraries with <5% overlapping sgRNA sequences for the PATU8902 and

PATU8988T screens to mitigate the possibility that genes identified were the consequence of off-target effects.

Screening was performed using a lentivirally delivered two-vector CRISPR-Cas9 system (Doench et al., 2016; Shalem et al., 2014). Specifically, Cas9-expressing cells were infected with either the genome scale CRISPR-Cas9 knockout (GeCKOv2) (Shalem et al., 2014) or Avana (Doench et al., 2016) sgRNA library, passaged for 7–10 d to allow for genomic editing, and treated with trametinib for 14 d (Figures 1A and S1E–F). We identified sgRNAs that became enriched in the trametinib-treated samples compared to the original pool of sgRNA plasmids by defining significant enrichment as a $\log_2$ fold-change of at least 4 standard deviations from the mean $\log_2$ fold-change of all sgRNAs ($p<10^{-4}$). A gene was considered a candidate modulator of trametinib sensitivity if over half of the sgRNAs targeting the gene were enriched. We found one gene in the high dose PATU8902 screen and 10 genes in the moderate dose PATU8988T screen that met this criterion (Figures 1B–C and Table S1). Since CIC loss was found to promote proliferation/survival in the context of trametinib treatment in both the high dose and moderate dose screens, we investigated how *CIC* knockout (CIC^{KO}) mediates trametinib resistance (Figure 1D).

CIC Loss Modulates Sensitivity to MEK and BRAF Inhibition in Multiple Contexts without Reactivating ERK Signaling

We tested 11 *CIC*-targeting sgRNAs to identify sgRNAs that effectively eliminated CIC expression, which included 3 of the 6 sgRNAs used in the PATU8902 screen, and all 4 of the sgRNAs used in the PATU8988T screen (Figure S2A). We found that all of the CIC-targeting sgRNAs that robustly depleted CIC were significantly enriched in the screens (Figure S2A). In addition, we assessed the ability of these sgRNAs to modulate trametinib sensitivity in the *NRAS*-mutant lung cancer cell line NCIH1299 using a short-term viability assay. We found that only the sgRNAs that effectively depleted CIC conferred resistance to trametinib treatment (Figure S2B). Subsequently, we verified that CIC loss conferred resistance to trametinib treatment in PATU8902 cells using a cell counting assay (Figures 2A–B).

We then assessed the ability of CIC^{KO} to modulate the response to MEK inhibition in several different lineage and mutational contexts. Cells were treated with the lowest concentration of inhibitor that robustly inhibited ERK phosphorylation (for MEK inhibitor) or MEK phosphorylation (for BRAF inhibitor) and induced proliferative arrest or cell death. Using a cell counting assay, we determined that CIC knockout modulated the response to trametinib treatment in the *KRAS*-mutant lung cancer cell line CALU1 (Figure 2C–D). In addition, using a long-term clonogenic proliferation assay, we found that CIC^{KO} also modulated the response to MEK inhibition in *KRAS*-mutant lung or colon cancer, to MEK inhibition in *NRAS*-mutant lung cancer or melanoma, and to MEK or BRAF inhibition in *BRAF*-mutant melanoma, lung cancer, and colon cancer cells (Figures 2E and S2C). CIC loss restored cell proliferation in the context of trametinib treatment, and CIC^{KO} cells treated with trametinib appeared morphologically comparable to CIC^{WT} cells treated with DMSO (Figure S2D). However, CIC^{KO} did not restore signaling through the MAPK or PI3K/AKT pathways as measured by phosphorylation of ERK or AKT (Figures 2B, 2D, and S3A–B).

Thus, deletion of *CIC* permitted the proliferation of cells expressing different RAS or MAPK pathway oncogenes in several lineages.

We next assessed whether CIC^{KO} allowed cells to proliferate in the context of KRAS depletion in PATU8902, a KRAS-dependent cell line. We generated the PATU8902 pTetK cell line, which harbors a doxycycline-inducible shRNA targeting *KRAS*. We transduced PATU8902 pTetK cells with a vector containing both Cas9 and an sgRNA targeting either *LacZ* or *CIC* to generate isogenic CIC^{WT} and CIC^{KO} variant cell lines (Figure 3A). We found that deleting *CIC* reduced sensitivity to KRAS depletion in PATU8902 pTetK cells in a long-term clonogenic proliferation assay (Figure 3B).

To determine whether proliferation mediated by *CIC* deletion was specific to inhibition of the MAPK pathway, we treated CIC^{KO} cells with the MEK inhibitor selumetinib or three cytotoxic chemotherapeutic agents. CIC^{KO} conferred resistance to selumetinib, but not to cisplatin, paclitaxel, or 5-FU (Figures 3C–F and S3D). These observations confirmed that CIC loss promotes proliferation/survival in the setting of suppressed MAPK signaling in several different epithelial lineages but does not promote survival to cytotoxic agents.

CIC Loss Reduces Sensitivity to Trametinib Treatment *In Vivo*

To determine whether CIC loss modulates the response to trametinib treatment *in vivo*, we implanted mice with PATU8902 CIC^{WT} or CIC^{KO} cells and initiated daily trametinib treatment after tumor formation. We found that CIC^{KO} had no effect on tumor growth *in vivo* (Figure 3G). Trametinib treatment decreased the growth of CIC^{WT} tumors compared to vehicle treatment ($p = 0.01$), but had little effect on CIC^{KO} tumors. Indeed, trametinib-treated CIC^{KO} tumors grew at comparable rates to vehicle-treated CIC^{WT} or CIC^{KO} tumors (Figure 3H). Based on these observations, we concluded that CIC^{KO} reduces sensitivity to trametinib treatment *in vivo*.

MEK Inhibition Increases CIC-mediated Repression of ETS Transcription Factors

CIC is a transcriptional repressor that is phosphorylated and inhibited by MAPK in *D. melanogaster* (Astigarraga et al., 2007; Dissanayake et al., 2011; Jiménez et al., 2000). 2 CIC isoforms (CIC-S and CIC-L), which differ in size and in their N-terminal region (Lam et al., 2006), exist. In flies, CIC-S fulfills most known CIC functions (Jiménez et al., 2012). We found that in all the cell lines we tested, trametinib treatment induced an increase in nuclear CIC-S (Figures 2B, 2D, and S4). In contrast, the effect of trametinib on CIC-L localization was inconsistent. Trametinib treatment decreased levels of nuclear CIC-L in HCC364, CALU1, and PATU8902 cells; increased levels of nuclear CIC-L in PATU8988T; and had no effect on levels of nuclear CIC-L in NCIH1299, HT29, and MELJUSO cells (Figures 2B, 2D, and S4). As CIC^{KO} confers resistance to trametinib treatment in all of these cell lines (Figures 2A, 2C, 2E and S2C) and only the localization of CIC-S is consistently altered by trametinib treatment across all cell lines, we concluded that decreased CIC-S in CIC^{KO} cells mediated resistance to trametinib.

Because CIC is a transcriptional repressor whose nuclear/cytoplasmic localization is regulated by MAPK signaling (Dissanayake et al., 2011; Jiménez et al., 2012), we hypothesized that MAPKi leads to active nuclear CIC and repression of pro-proliferative

CIC target genes and that loss of CIC would restore expression of these genes, reducing sensitivity to MAPKi. To identify the relevant CIC target genes, we treated control CIC^{WT} (sgGFP-1) or CIC^{KO} (sgCIC-1 or sgCIC-2) cells from 4 cell lines of different lineages that harbor different RAS-pathway mutations with DMSO or trametinib for 24 h and performed RNA-sequencing (Figures 4A and S5A). We analyzed the gene expression profiles to identify genes whose expression was suppressed in CIC^{WT} cells treated with trametinib and restored in CIC^{KO} cells treated with trametinib. We found that trametinib treatment reduces the expression of all 3 members of the PEA3 family of ETS transcription factors (ETV1, ETV4, and ETV5) in all cell lines, and that loss of CIC results in maintained expression of at least one of these genes despite MEK inhibition (Figures 4B, S5B and Table S2).

We confirmed that trametinib treatment robustly suppressed ETV1, 4, and 5 mRNA (Figures 4C–D, S5C–D) and protein (Figure S5E) expression in CIC^{WT} cells and that ETV 1, 4, and 5 expression was partially restored in CIC^{KO} cells. These observations suggest that active nuclear CIC represses ETV1, 4, and 5 expression in multiple cell lineages. We concluded that signaling through the MAPK pathway induces ETV1, 4, and 5 expression by reducing nuclear CIC-S, relieving CIC-mediated gene repression. We hypothesized that elevated ETV1, 4, and 5 expression may be responsible for the resistance phenotype in CIC^{KO} cells.

Increased Expression of ETV Transcription Factors is Necessary and Sufficient to Modulate the Response to MEK Inhibition

To assess whether expression of ETV1, 4, or 5 is necessary for the observed proliferation in the presence of MAPKi conferred by *CIC* deletion, we suppressed ETV1, 4, or 5 expression in CIC^{WT} or CIC^{KO} cells (Figure S6A–B). We used long-term proliferation assays to determine the effect of ETV1, 4, or 5 depletion on cell proliferation/survival in the context of trametinib treatment. We found that expression of ETV1, 4, and 5 was necessary for the full resistance mediated by CIC loss (Figure 5A).

To determine if overexpression of ETV1, 4, or 5 was sufficient to restore proliferation in the presence of MEK inhibition, we exogenously expressed LacZ (control), ETV1, ETV4-S (short isoform), ETV4-L (long isoform) or ETV5 and treated cells with DMSO or trametinib (Figures 5B and S6C). Overexpression of ETV1, ETV4-S, ETV4-L, or ETV5 permitted proliferation in the setting of MEK inhibition in CALU1, PATU8902 and PATU8988T cells (Figures 5C, S6D). These observations extend a prior finding that ETV1 overexpression conferred resistance to MAPKi in *BRAF*-mutant melanoma (Johannessen et al., 2013). These findings suggest that increased expression of ETV1, 4, and 5 in CIC^{KO} cells is necessary for the effects mediated by CIC^{KO}, and that overexpression of ETV1, 4, or 5 suffices to reduce sensitivity to MEK inhibition.

ATXN1L Deletion Modulates Trametinib Sensitivity by Reducing CIC Protein

In mice, ATXN1L has been shown to form a complex with CIC and increase CIC protein expression (Bowman et al., 2007; Crespo-Barreto et al., 2010; Lee et al., 2011), and ATXN1L has been implicated as a co-repressor that synergistically enhances CIC transcriptional repressor activity (Crespo-Barreto et al., 2010; Lee et al., 2011). When we examined the top scoring genes in our screens, we noticed that in the moderate dose

PATU8988T screen, all 4 sgRNAs targeting *ATXN1L* were enriched >2 SD from the mean ($p<0.05$, Figure 1C and Table S1). In the high dose PATU8902 screen, all 6 sgRNAs targeting *ATXN1L* were enriched (Figure 1B and Table S1). We hypothesized that *ATXN1L* deletion may promote increased proliferation/survival in the context of trametinib treatment by reducing CIC expression and/or repressive function.

We generated $ATXN1L^{KO}$ cells and assessed the efficiency of *ATXN1L* knockout by TIDE (Tracking of Indels by DEcomposition, Brinkman et al., 2014), a method to quantify the frequency of mutations induced by CRISPR-Cas9, as we were unable to identify an ATXN1L-specific antibody for immunoblotting (Figure S7). In brief, the region around the sgRNA editing site is PCR amplified from genomic DNA and sequenced, compared to one derived from a control cell line (sgLacZ-1), and the frequency of genome editing is estimated by the proportion of aberrant base signals of the test sequencing trace compared to the control sequencing trace. We found that *ATXN1L* was effectively modified in >50% of CALU1, PATU8902, and PATU8988T cells expressing sgATXN1L, but in <2.2% of PATU8988T cells expressing sgLacZ (Figure S7A).

ATXN1L loss had no effect on baseline CIC expression at the transcriptional level (Figure 6A). However, upon trametinib treatment, we noted that $ATXN1L^{WT}$ cells slightly upregulated CIC mRNA expression while $ATXN1L^{KO}$ cells did not (Figure 6A). Notably, $ATXN1L^{KO}$ cells exhibited reduced expression of CIC-S protein at baseline and upon trametinib treatment (Figure 6B). These observations suggest that ATXN1L increases CIC expression post-translationally (Bowman et al., 2007; Crespo-Barreto et al., 2010; Lee et al., 2011).

We found that *ATXN1L* deletion reduced sensitivity to MEK inhibition by trametinib or selumetinib (Figures 6C and S7D). To identify the relevant ATXN1L target genes that modulate sensitivity to MEK inhibition, we treated control $ATXN1L^{WT}$ (sgLacZ-1) or $ATXN1L^{KO}$ (sgATXN1L-1 or sgATXN1L-2) cells with DMSO or trametinib for 24 h, and performed RNA-sequencing (Figure 7A). We looked for genes whose expression was suppressed in $ATXN1L^{WT}$ cells treated with trametinib and restored in $ATXN1L^{KO}$ cells treated with trametinib. We found that trametinib treatment decreased expression of ETV1, ETV4, and ETV5; and that loss of ATXN1L restored expression of at least one of these genes in the context of MEK inhibition (Figures 7B and S7E, and Table S3). $ATXN1L^{KO}$ partially restored ETV1, 4, and 5 mRNA expression in trametinib-treated cells, albeit not to the same magnitude as CIC^{KO} cells (Figure 7C). These observations suggest that loss of ATXN1L mediates resistance to MEK inhibition by reducing CIC levels, which permits increased expression of ETV1, 4, and 5.

We propose a model in which oncogenic MAPK signaling in *RAS*- or *BRAF*-mutant cells constitutively inactivates CIC. Upon MEK or BRAF inhibition, active CIC represses ETV1, 4, and 5 expression. CIC loss modulates the response to trametinib and vemurafenib treatment by restoring expression of the ETV transcription factors at a transcriptional level. Deletion of *ATXN1L* modulates the response to MEK inhibition by reducing CIC protein levels and restoring expression of ETV1, 4, and 5 (Figure 7D).

Low *ATXN1L* Expression is Associated With Poor Overall Survival in *BRAF*-mutant Melanoma Treated with MAPK-pathway Inhibitors

To determine whether the expression of *CIC* or *ATXN1L* correlated with intrinsic resistance to MAPK pathway inhibitor therapy in cancers with mutations in the MAPK pathway, we analyzed pre-treatment microarray expression data from 30 $BRAF^{V600}$-mutant melanoma metastases derived from 21 patients subsequently treated with dabrafenib or vemurafenib (Rizos et al., 2014) and 9 patients treated with the combination of dabrafenib and trametinib (Long et al., 2014). We categorized the 10 tumors with lowest or highest *ATXN1L* expression as 'low' or 'high' *ATXN1L* expressers, respectively, and found that low pre-treatment *ATXN1L* expression correlated with decreased overall survival ($p = 0.0375$, Figure 7E). This observation suggests that lower *ATXN1L* expression marks tumors with intrinsic resistance to BRAF or MEK inhibitor therapy in *BRAF*-mutant melanoma.

DISCUSSION

The MAPK pathway mediates cellular responses by altering gene expression through direct phosphorylation of several nuclear factors. Although more than 150 substrates of ERK1/2 have been identified (Yoon and Seger, 2006), which of these substrates play key roles in oncogenic and treatment-related contexts remains unclear. Here, we identify CIC as an important effector of MAPK in the setting of MAPKi. ERK-dependent phosphorylation of upstream components of the pathway such as EGFR, SOS, and RAF (Buday et al., 1995; Dougherty et al., 2005; Heisermann et al.; Li et al., 2008; Porfiri and McCormick, 1996; Ritt et al., 2010) dampens MAPK pathway activity. In addition, ERK signaling induces the expression of SPRY and SPRY-related proteins with an EVH1 domain (SPRED) proteins (Kim and Bar-Sagi, 2004), which inhibit MAPK signaling at multiple levels of the pathway, as well as DUSP phosphatases (Owens and Keyse, 2007), which directly dephosphorylate and inhibit ERK1/2. The existence of multiple regulators, including CIC, allows for precise modulation of the magnitude and duration of MAPK signaling in different contexts.

We observed that deletion of several negative regulators of the MAPK pathway (*RASA2, SPRY2*, *DUSP1*, and *DUSP7*) also conferred trametinib resistance to PATU8988T cells (Table S1). However, loss of CIC modulated the response to trametinib treatment in a more robust and consistent manner. Certain negative regulators of the MAPK pathway, such as SPRY and DUSP proteins, may not have reduced sensitivity to MEK inhibition in the CRISPR-Cas9 screens due to the presence of functionally redundant family members. We conclude that the CIC-ETS transcription factor axis is an important modulator of MAPK pathway output across cancer cells of multiple lineages whose proliferation is dependent on oncogenic MAPK signaling.

In *D. melanogaster*, Cic is a well-characterized repressor of EGFR-Ras-MAPK signaling that prevents aberrant cell proliferation by downregulating ETS factors in the absence of MAPK signaling (Jiménez et al., 2012; Jin et al., 2015). A prior study suggested that this role is conserved in human CIC (Dissanayake et al., 2011). CIC alterations have been reported in several cancer types. The majority of oligodendrogliomas harbor inactivating CIC mutations (Bettegowda et al., 2011) and, consequently, overexpress the ETV transcription factors (Padul et al., 2015). *CIC-DUX4* translocations, which encode a fusion

protein that upregulates expression of ETV1 and ETV5, have been identified in Ewings sarcoma (Kawamura-Saito et al., 2006). Indeed, we noted that tumors formed by *CIC*^{KO} cells were larger, suggesting that loss of CIC may also contribute to tumor formation *in vivo*. In recent work, CIC loss was found to promote metastases in a lung cancer model (Okimoto et al., 2017).

Our observations indicate that the PEA3 family of ETS transcription factors, which are negatively regulated by CIC, may be key nuclear effectors of oncogenic MAPK signaling. Indeed, a prior study suggested that ETS transcription factors may activate a RAS/MAPK transcriptional program in the absence of MAPK pathway (Hollenhorst et al., 2011). We note that RFWD2 (COP1), DET1 and DDA1, substrate receptors of the CRL4$^{COP1/DET1}$ E3 ubiquitin ligase (Wertz et al., 2004) that have been reported to mediate the ubiquitination and degradation of ETV1, 4, and 5 (Baert et al., 2010; Vitari et al., 2011) and c-Jun (Bianchi et al., 2003), were also hits in the PATU8988T screen (Figure 1D). We found that while overexpression of a single ETS transcription factor conferred resistance to trametinib, suppression of ETV1, 4, or 5 alone strongly decreased the resistance conferred by *CIC* deletion. These observations suggest that elevated global expression of ETS transcription factors modulates the response to MEK inhibitor treatment. We found that the exogenously expressed ETS transcription factors were overexpressed at levels greater than was achieved by *CIC*^{KO}, and it is possible that a single ETS transcription factor is sufficient to confer resistance at high levels of expression while at moderate levels, such as that conferred by *CIC*^{KO}, a combination of several ETS transcription factors is necessary.

Atxn1l$^{-/-}$ mice exhibit defective lung alveolarization, attributed to destabilization of Cic and derepression of *Etv1* and *Etv4*, which increases expression of several matrix metalloproteinase (*Mmp*) genes (Lee et al., 2011). Several reports indicate that ATXN1L enhances CIC function by stabilizing post-transcriptional CIC expression and by working as a transcriptional co-repressor with CIC (Bowman et al., 2007; Crespo-Barreto et al., 2010; Lee et al., 2011). Although ATXN1L has been reported to suppress *HEY1* expression (Tong et al., 2011), the phenotype seen in *Atxn1l*$^{-/-}$ mice suggests that the major role of ATXN1L is to augment CIC-mediated gene repression; however, it remains possible that deletion of *ATXN1L* affects other pathways that contribute to tumor growth together with those mediated by CIC.

We found that *CIC* deletion reduced sensitivity to trametinib treatment in both *in vitro* and *in vivo*. Observations from *in vitro* clonogenic proliferation assays suggest that *CIC* or *ATXN1L* deletion and ETV1/4/5 overexpression may also modulate *in vivo* sensitivity to MAPKi in *RAS*- or *BRAF*-mutant tumors or to KRAS depletion in KRAS-dependent tumors. However, it is possible that the reduction in sensitivity to MAPKi conferred by *CIC* or *ATXN1L* deletion and ETV1/4/5 overexpression is more robust *in vitro* than *in vivo*.

The majority of acquired resistance mechanisms to MAPK pathway inhibitor therapy that have been identified in patients with *RAF*-mutant cancers involve upregulation of MAPK pathway signaling upstream of ERK (Long et al., 2014; Rizos et al., 2014; Shi et al., 2014; Van Allen et al., 2014; Wagle et al., 2011; 2014). Our observations suggest that, if RAF/MEK signaling is sufficiently suppressed in tumors with mutant *RAS* or *BRAF*,

acquired resistance may arise from altered transcriptional output mediated by aberrant expression of transcription factors activated downstream of MAPK, such as ETV1, 4, and 5. Dysregulation of these transcription factors downstream of ERK may also promote intrinsic resistance to inhibition of the MAPK pathway.

Our observations suggest that low ATXN1L activity, which results in reduced CIC protein as well as elevated ETS transcription factor expression in the context of MAPKi, may be a mechanism of intrinsic resistance to MAPK inhibitor therapy in *BRAF*-mutant melanoma. We found that low *ATXN1L* expression in *BRAF*-mutant melanoma correlated with decreased overall survival in patients treated with MAPKi. However, we did not observe a correlation between low *CIC* expression and poor survival outcome. This could be attributable to technical or biological reasons. Since gene expression in tumor samples was determined by bead-based microarrays, it is possible that the CIC probe was insufficiently sensitive to distinguish between high and low CIC expression. Alternatively, total *CIC* mRNA expression may not reflect nuclear CIC-S protein levels, which may be a more relevant marker of sensitivity to MAPKi. In addition, ETV1, 4, and 5 expression were not predictive of survival outcome, likely because oncogenic BRAF signaling inhibits CIC and induces high ETV1, 4, and 5 expression in all tumor samples, making ETV1, 4, and 5 expression an insensitive readout of ATXN1L-CIC-ETS transcription factor pathway activity in pre-treatment samples.

BRAF and MEK inhibitors are currently being tested in clinical trials for *RAS*-mutant and *BRAF*-mutant cancers. However, pre-treatment and post-relapse biopsy specimens for molecular analysis of resistance mechanisms are not accessible for most of these trials. Moreover, most available samples from patients treated with single agent MEK or BRAF inhibitor therapies have shown only partial suppression of the MAPK signaling pathway with these agents at clinically tolerable doses. We propose that altered transcriptional output downstream of MAPK signaling may represent an important resistance mechanism upon full suppression of the canonical kinase signaling pathway. Thus, even the limited number of available clinical samples may not be sufficient to determine whether CIC loss is an operant mechanism of intrinsic or acquired resistance in these clinical settings. However, stratifying patients for treatment based on ATXN1L-CIC-ETS transcription factor pathway activity level may also allow for the selection of patients more likely to respond to MEK and BRAF inhibitors.

EXPERIMENTAL PROCEDURES

For additional details, see the Extended Experimental Procedures.

Cell Lines and Reagents

Cell lines, culture conditions, and sources of sgRNA and shRNA plasmids, expression plasmids, and antibodies are described in the Supplemental Experimental Procedures.

Genome Scale CRISPR-Cas9 Resistance Screens

Libraries and protocols for the genome scale CRISPR-Cas9 knockout screen are described in the Supplemental Experimental Procedures.

Drug Titration for Cell Counting and Long-term Clonogenic Proliferation Assays

CALU1, HCC364, HCT116, and NCIH1299 cells were treated with at least 5 different concentrations of drug (trametinib, selumetinib, or vemurafenib) for 24 h, and phospho-ERK levels were assessed by immunoblot analysis. The concentration of drug that fully inhibited phospho-ERK levels was used in subsequent assays. The trametinib and vemurafenib doses used for A375 correspond to published IC50 values (Boussemart et al., 2014).

Short-term Viability Assay

Protocol for short-term viability assay is described in the Supplemental Experimental Procedures.

Cell Counting Assay

Cells were seeded in 10 cm (1–2 × 10^6 cells) or 15 cm (1–3 × 10^6 cells) plates and treated with drug or DMSO as indicated. Cells were passaged or media was refreshed every 3–4 d. Cells were counted at each passage, and number of cell doublings was calculated.

Long-term Clonogenic Proliferation Assay

Cells were seeded in 12- or 24-well plates at a density of 5,000–20,000 cells per well and treated with drug or DMSO. Cells were exposed to DMSO for 6–9 d, and to drug or doxycycline (PATU8902 pTetK cells) for 9–18 d, with media changed every 3 d. Cells were fixed with 10% formalin and stained with 0.5% crystal violet in 10% ethanol for 20 min. After acquiring images, crystal violet uptake was extracted with 10% acetic acid and quantified by measuring absorbance at 565 nm using a SpectraMax M5 microplate reader (Molecular Devices).

In vivo Xenografts

All procedures were performed according to protocols approved by the Institutional Animal Care and Use Committees of the Dana-Farber Cancer Institute. The mouse xenograft studies are described in the Supplemental Experimental Procedures.

RNA-sequencing

sgGFP and sgCIC cells—200,000 – 400,000 cells were seeded in 4 wells of a 6-well plate and allowed to adhere overnight. Subsequently, 2 wells were treated with DMSO and 2 wells were treated with trametinib (A375: 1 nM, CALU1: 50 nM, HCT116: 50 nM, PATU8902: 100 nM) for 24 h. Total RNA was extracted using an RNeasy kit (Qiagen). First strand cDNA was generated from 1.5 μg of total RNA using Oligo(dT)12–19 Primer (Invitrogen) and AffinityScript Multiple Temperature Reverse Transcriptase (Agilent). Second strand cDNA was synthesized using an mRNA Second Strand Synthesis Module (#6111L) and washed with Agencourt AMPure XP beads (Beckman Coulter). Libraries were prepared by tagmentation (Nextera XT DNA Sample Preparation Kit, Illumina) using index primers (Nextera XT Index kit, Illumina) to facilitate multiplexing.

sgGFP and sgATXN1L cells—200,000 – 400,000 cells were seeded in 4 wells of a 6-well plate and allowed to adhere overnight. Subsequently, 2 wells were treated with DMSO

and 2 wells were treated with trametinib (PATU8902: 50nM, PATU8988T: 50 nM) for 24 h. Total RNA was extracted using an RNeasy kit (Qiagen). RNA sequencing libraries were prepared using a NEBNext Ultra Directional RNA Library Prep Kit for Illumina, NEB E7420.

The concentration of each cDNA library was quantified with the KAPA Illumina ABI Quantification Kit (Kapa Biosystems). Libraries were pooled for sequencing using the HiSeq 2500. Reads were mapped to the reference human genome (hg19) using Tophat 2.0.11. Transcript assembly, abundance estimation, and differential expression analysis were performed with Cufflinks 2.0.2. Two replicates for each cell line/genetic perturbation/ treatment were grouped to derive significance of differential expression across experimental conditions.

Quantitative PCR and Tracking of Indels by DEcomposition (TIDE)

Protocol and primers used for quantitative PCR and TIDE are presented in the Supplemental Experimental Procedures.

Melanoma Outcome Data Analysis

Data from 30 *BRAF*^{V600}-mutant melanoma metastases derived from 21 patients treated with dabrafenib or vemurafenib (Rizos et al., 2014) and 9 patients treated with the combination of dabrafenib and trametinib (Long et al., 2014) was analyzed. Patients were grouped by pre-treatment *ATXN1L* expression, where 'High *ATXN1L*' and 'Low ATXN1L' groups include the 10 patients with highest or lowest *ATXN1L* expression in the cohort of 30 patients, respectively.

Statistical Methods

Statistical analysis for cell counting assays, long-term clonogenic proliferation assays, and quantitative PCR were performed using Prism GraphPad. Statistical analysis for RNA sequencing was performed using Cufflinks 2.0.2. Statistical significance for xenograft experiments was determined by ANOVA and paired t-test. Statistical significance for melanoma outcome data analysis was calculated using the log-rank (Mantel-Cox) test.

Supplementary Material

Refer to Web version on PubMed Central for supplementary material.

Acknowledgments

We thank Eejung Kim, David Takeda, Ole Gjoerup, Yaara Zwang, and Mikael Rinne for helpful discussions. This project was supported by R01 CA130988 (W.C.H.), U01 CA199253 (W.C.H.), U01 CA176058 (W.C.H.), P01 CA154303 (W.C.H), and P50 CA127003 (W.C.H. and A.J.A.). E.B.K. was supported by postdoctoral fellowships from the Hope Funds for Cancer Research (HFCR-11-03-03) and NIH F32 (CA189306). A.J.A. was supported by the Pancreatic Cancer Action Network Samuel Stroum Fellowship, Hope Funds for Cancer Research Postdoctoral Fellowship, American Society of Clinical Oncology Young Investigator Award, Dana Farber Cancer Institute Hale Center for Pancreatic Cancer, Perry S. Levy Endowed Fellowship, and the Harvard Catalyst and Harvard Clinical and Translational Science Center (UL1 TR001102). J.G.D. was supported by the Next Generation Fund at the Broad Institute. W.C.H. is a consultant and receives research support from Novartis.

References

Astigarraga S, Grossman R, Díaz-Delfín J, Caelles C, Paroush Z, Jiménez G. A MAPK docking site is critical for downregulation of Capicua by Torso and EGFR RTK signaling. The EMBO Journal. 2007; 26:668–677. [PubMed: 17255944]

Baert JL, Monte D, Verreman K, Degerny C, Coutte L, de Launoit Y. The E3 ubiquitin ligase complex component COP1 regulates PEA3 group member stability and transcriptional activity. Oncogene. 2010; 29:1810–1820. [PubMed: 20062082]

Bettegowda C, Agrawal N, Jiao Y, Sausen M, Wood LD, Hruban RH, Rodriguez FJ, Cahill DP, McLendon R, Riggins G, et al. Mutations in CIC and FUBP1 contribute to human oligodendroglioma. Science. 2011; 333:1453–1455. [PubMed: 21817013]

Bianchi E, Denti S, Catena R, Rossetti G, Polo S, Gasparian S, Putignano S, Rogge L, Pardi R. Characterization of human constitutive photomorphogenesis protein 1, a RING finger ubiquitin ligase that interacts with Jun transcription factors and modulates their transcriptional activity. J Biol Chem. 2003; 278:19682–19690. [PubMed: 12615916]

Blasco RB, Francoz S, Santamaría D, Cañamero M, Dubus P, Charron J, Baccarini M, Barbacid M. c-Raf, but not B-Raf, is essential for development of K-Ras oncogene-driven non-small cell lung carcinoma. Cancer Cell. 2011; 19:652–663. [PubMed: 21514245]

Blumenschein G, Smit EF, Planchard D, Kim D-W, Cadranel J, De Pas T, Dunphy F, Udud K, Ahn M-J, Hanna NH, et al. A randomized phase 2 study of the MEK1/MEK2 inhibitor trametinib (GSK1120212) compared with docetaxel in KRAS-mutant advanced non-small cell lung cancer (NSCLC). Ann Oncol. 2015

Boussemart L, Malka-Mahieu H, Girault I, Allard D, Hemmingsson O, Tomasic G, Thomas M, Basmadjian C, Ribeiro N, Thuaud F, et al. eIF4F is a nexus of resistance to anti-BRAF and anti-MEK cancer therapies. Nature. 2014; 513:105–109. [PubMed: 25079330]

Bowman AB, Lam YC, Jafar-Nejad P, Chen HK, Richman R, Samaco RC, Fryer JD, Kahle JJ, Orr HT, Zoghbi HY. Duplication of Atxn1l suppresses SCA1 neuropathology by decreasing incorporation of polyglutamine-expanded ataxin-1 into native complexes. Nat Genet. 2007; 39:373–379. [PubMed: 17322884]

Brinkman EK, Chen T, Amendola M, van Steensel B. Easy quantitative assessment of genome editing by sequence trace decomposition. Nucleic Acids Research. 2014; 42:e168. [PubMed: 25300484]

Buday L, Warne PH, Downward J. Downregulation of the Ras activation pathway by MAP kinase phosphorylation of Sos. Oncogene. 1995; 11:1327–1331. [PubMed: 7478553]

Caunt CJ, Sale MJ, Smith PD, Cook SJ. MEK1 and MEK2 inhibitors and cancer therapy: the long and winding road. Nat Rev Cancer. 2015; 15:577–592. [PubMed: 26399658]

Chapman PB, Hauschild A, Robert C, Haanen JB, Ascierto P, Larkin J, Dummer R, Garbe C, Testori A, Maio M, et al. Improved Survival with Vemurafenib in Melanoma with BRAF V600E Mutation. N Engl J Med. 2011; 364:2507–2516. [PubMed: 21639808]

Chien Y, Kim S, Bumeister R, Loo YM, Kwon SW, Johnson CL, Balakireva MG, Romeo Y, Kopelovich L, Gale M, et al. RalB GTPase-mediated activation of the IkappaB family kinase TBK1 couples innate immune signaling to tumor cell survival. Cell. 2006; 127:157–170. [PubMed: 17018283]

Collisson EA, Trejo CL, Silva JM, Gu S, Korkola JE, Heiser LM, Charles RP, Rabinovich BA, Hann B, Dankort D, et al. A central role for RAF→MEK→ERK signaling in the genesis of pancreatic ductal adenocarcinoma. Cancer Discovery. 2012; 2:685–693. [PubMed: 22628411]

Corcoran RB, Ebi H, Turke AB, Coffee EM, Nishino M, Cogdill AP, Brown RD, Pelle Della P, Dias-Santagata D, Hung KE, et al. EGFR-mediated reactivation of MAPK signaling contributes to insensitivity of BRAF mutant colorectal cancers to RAF inhibition with vemurafenib. Cancer Discovery. 2012; 2:227–235. [PubMed: 22448344]

Cox AD, Fesik SW, Kimmelman AC, Luo J, Der CJ. Drugging the undruggable RAS: Mission Possible? Nature Publishing Group. 2014; 13:828–851.

Crespo-Barreto J, Fryer JD, Shaw CA, Orr HT, Zoghbi HY. Partial loss of ataxin-1 function contributes to transcriptional dysregulation in spinocerebellar ataxia type 1 pathogenesis. PLoS Genet. 2010; 6:e1001021. [PubMed: 20628574]

Dissanayake K, Toth R, Blakey J, Olsson O, Campbell DG, Prescott AR, MacKintosh C. ERK/p90(RSK)/14-3-3 signalling has an impact on expression of PEA3 Ets transcription factors via the transcriptional repressor capicúa. Biochem J. 2011; 433:515–525. [PubMed: 21087211]

Doench JG, Fusi N, Sullender M, Hegde M, Vaimberg EW, Donovan KF, Smith I, Tothova Z, Wilen C, Orchard R, et al. Optimized sgRNA design to maximize activity and minimize off-target effects of CRISPR-Cas9. Nature Biotechnology. 2016

Dougherty MK, Müller J, Ritt DA, Zhou M, Zhou XZ, Copeland TD, Conrads TP, Veenstra TD, Lu KP, Morrison DK. Regulation of Raf-1 by Direct Feedback Phosphorylation. Molecular Cell. 2005; 17:215–224. [PubMed: 15664191]

Duncan JS, Whittle MC, Nakamura K, Abell AN, Midland AA, Zawistowski JS, Johnson NL, Granger DA, Jordan NV, Darr DB, et al. Dynamic reprogramming of the kinome in response to targeted MEK inhibition in triple-negative breast cancer. Cell. 2012; 149:307–321. [PubMed: 22500798]

Hatzivassiliou G, Song K, Yen I, Brandhuber BJ, Anderson DJ, Alvarado R, Ludlam MJC, Stokoe D, Gloor SL, Vigers G, et al. RAF inhibitors prime wild-type RAF to activate the MAPK pathway and enhance growth. Nature. 2010; 464:431–435. [PubMed: 20130576]

Heidorn SJ, Milagre C, Whittaker S, Nourry A, Niculescu-Duvas I, Dhomen N, Hussain J, Reis-Filho JS, Springer CJ, Pritchard C, et al. Kinase-dead BRAF and oncogenic RAS cooperate to drive tumor progression through CRAF. Cell. 2010; 140:209–221. [PubMed: 20141835]

Heisermann, GJ., Wiley, HS., Walsh, BJ., Ingraham, HA., Fiol, CJ., Gill, GN. Mutational removal of the Thr669 and Ser671 phosphorylation sites alters substrate specificity and ligand-induced internalization of the epidermal growth factor receptor. Jbc.org

Hollenhorst PC, Ferris MW, Hull MA, Chae H, Kim S, Graves BJ. Oncogenic ETS proteins mimic activated RAS/MAPK signaling in prostate cells. Genes & Development. 2011; 25:2147–2157. [PubMed: 22012618]

Hyman DM, Puzanov I, Subbiah V, Faris JE, Chau I, Blay J-Y, Wolf J, Raje NS, Diamond EL, Hollebecque A, et al. Vemurafenib in Multiple Nonmelanoma Cancers with BRAF V600 Mutations. N Engl J Med. 2015; 373:726–736. [PubMed: 26287849]

Infante JR, Fecher LA, Falchook GS, Nallapareddy S, Gordon MS, Becerra C, DeMarini DJ, Cox DS, Xu Y, Morris SR, et al. Safety, pharmacokinetic, pharmacodynamic, and efficacy data for the oral MEK inhibitor trametinib: a phase 1 dose-escalation trial. Lancet Oncol. 2012; 13:773–781. [PubMed: 22805291]

Jiménez G, Guichet A, Ephrussi A, Casanova J. Relief of gene repression by torso RTK signaling: role of capicua in Drosophila terminal and dorsoventral patterning. Genes & Development. 2000; 14:224–231. [PubMed: 10652276]

Jiménez G, Shvartsman SY, Paroush Z. The Capicua repressor--a general sensor of RTK signaling in development and disease. J Cell Sci. 2012; 125:1383–1391. [PubMed: 22526417]

Jin Y, Ha N, Forés M, Xiang J, Gläßer C, Maldera J, Jiménez G, Edgar BA. EGFR/Ras Signaling Controls Drosophila Intestinal Stem Cell Proliferation via Capicua-Regulated Genes. PLoS Genet. 2015; 11:e1005634. [PubMed: 26683696]

Johannessen CM, Boehm JS, Kim SY, Thomas SR, Wardwell L, Johnson LA, Emery CM, Stransky N, Cogdill AP, Barretina J, et al. COT drives resistance to RAF inhibition through MAP kinase pathway reactivation. Nature. 2010; 468:968–972. [PubMed: 21107320]

Johannessen CM, Johnson LA, Piccioni F, Townes A, Frederick DT, Donahue MK, Narayan R, Flaherty KT, Wargo JA, Root DE, et al. A melanocyte lineage program confers resistance to MAP kinase pathway inhibition. Nature. 2013; 504:138–142. [PubMed: 24185007]

Kawamura-Saito M, Yamazaki Y, Kaneko K, Kawaguchi N, Kanda H, Mukai H, Gotoh T, Motoi T, Fukayama M, Aburatani H, et al. Fusion between CIC and DUX4 up-regulates PEA3 family genes in Ewing-like sarcomas with t(4;19)(q35;q13) translocation. Human Molecular Genetics. 2006; 15:2125–2137. [PubMed: 16717057]

Kim HJ, Bar-Sagi D. Modulation of signalling by Sprouty: a developing story. Nat Rev Mol Cell Biol. 2004; 5:441–450. [PubMed: 15173823]

Lam YC, Bowman AB, Jafar-Nejad P, Lim J, Richman R, Fryer JD, Hyun ED, Duvick LA, Orr HT, Botas J, et al. ATAXIN-1 interacts with the repressor Capicua in its native complex to cause SCA1 neuropathology. Cell. 2006; 127:1335–1347. [PubMed: 17190598]

Lee Y, Fryer JD, Kang H, Crespo-Barreto J, Bowman AB, Gao Y, Kahle JJ, Hong JS, Kheradmand F, Orr HT, et al. ATXN1 protein family and CIC regulate extracellular matrix remodeling and lung alveolarization. Developmental Cell. 2011; 21:746–757. [PubMed: 22014525]

Li X, Huang Y, Jiang J, Frank SJ. ERK-dependent threonine phosphorylation of EGF receptor modulates receptor downregulation and signaling. Cellular Signalling. 2008; 20:2145–2155. [PubMed: 18762250]

Lito P, Rosen N, Solit DB. Tumor adaptation and resistance to RAF inhibitors. Nat Med. 2013; 19:1401–1409. [PubMed: 24202393]

Long GV, Fung C, Menzies AM, Pupo GM, Carlino MS, Hyman J, Shahheydari H, Tembe V, Thompson JF, Saw RP, et al. Increased MAPK reactivation in early resistance to dabrafenib/trametinib combination therapy of BRAF-mutant metastatic melanoma. Nat Commun. 2014; 5:5694. [PubMed: 25452114]

Nazarian R, Shi H, Wang Q, Kong X, Koya RC, Lee H, Chen Z, Lee MK, Attar N, Sazegar H, et al. Melanomas acquire resistance to B-RAF(V600E) inhibition by RTK or N-RAS upregulation. Nature. 2010; 468:973–977. [PubMed: 21107323]

Nikolaev SI, Rimoldi D, Iseli C, Valsesia A, Robyr D, Gehrig C, Harshman K, Guipponi M, Bukach O, Zoete V, et al. Exome sequencing identifies recurrent somatic MAP2K1 and MAP2K2 mutations in melanoma. Nat Genet. 2011; 44:133–139. [PubMed: 22197931]

Okimoto RA, Breitenbuecher F, Olivas VR, Wu W, Gini B, Hofree M, Asthana S, Hrustanovic G, Flanagan J, Tulpule A, Blakely CM, Haringsma HJ, Simmons AD, Gowen K, Suh J, Miller VA, Ali S, Schuler M, Bivona TG. Inactivation of Capicua drives cancer metastasis. Nat Genet. 2017; 49:87–96. DOI: 10.1038/ng.3728 [PubMed: 27869830]

Owens DM, Keyse SM. Differential regulation of MAP kinase signalling by dual-specificity protein phosphatases. Oncogene. 2007; 26:3203–3213. [PubMed: 17496916]

Padul V, Epari S, Moiyadi A, Shetty P, Shirsat NV. ETV/Pea3 family transcription factor-encoding genes are overexpressed in CIC-mutant oligodendrogliomas. Genes Chromosomes Cancer. 2015

Porfiri E, McCormick F. Regulation of epidermal growth factor receptor signaling by phosphorylation of the ras exchange factor hSOS1. J Biol Chem. 1996; 271:5871–5877. [PubMed: 8621459]

Poulikakos PI, Persaud Y, Janakiraman M, Kong X, Ng C, Moriceau G, Shi H, Atefi M, Titz B, Gabay MT, et al. RAF inhibitor resistance is mediated by dimerization of aberrantly spliced BRAF(V600E). Nature. 2011; 480:387–390. [PubMed: 22113612]

Ritt DA, Monson DM, Specht SI, Morrison DK. Impact of feedback phosphorylation and Raf heterodimerization on normal and mutant B-Raf signaling. Molecular and Cellular Biology. 2010; 30:806–819. [PubMed: 19933846]

Rizos H, Menzies AM, Pupo GM, Carlino MS, Fung C, Hyman J, Haydu LE, Mijatov B, Becker TM, Boyd SC, et al. BRAF Inhibitor Resistance Mechanisms in Metastatic Melanoma: Spectrum and Clinical Impact. Clinical Cancer Research. 2014; 20:1965–1977. [PubMed: 24463458]

Shalem O, Sanjana NE, Hartenian E, Shi X, Scott DA, Mikkelsen TS, Heckl D, Ebert BL, Root DE, Doench JG, et al. Genome-scale CRISPR-Cas9 knockout screening in human cells. Science. 2014; 343:84–87. [PubMed: 24336571]

Shi H, Hugo W, Kong X, Hong A, Koya RC, Moriceau G, Chodon T, Guo R, Johnson DB, Dahlman KB, et al. Acquired resistance and clonal evolution in melanoma during BRAF inhibitor therapy. Cancer Discovery. 2014; 4:80–93. [PubMed: 24265155]

Stephen AG, Esposito D, Bagni RK, McCormick F. Dragging ras back in the ring. Cancer Cell. 2014; 25:272–281. [PubMed: 24651010]

Das Thakur M, Salangsang F, Landman AS, Sellers WR, Pryer NK, Levesque MP, Dummer R, McMahon M, Stuart DD. Modelling vemurafenib resistance in melanoma reveals a strategy to forestall drug resistance. Nature. 2013; 494:251–255. [PubMed: 23302800]

Tong X, Gui H, Jin F, Heck BW, Lin P, Ma J, Fondell JD, Tsai CC. Ataxin-1 and Brother of ataxin-1 are components of the Notch signalling pathway. EMBO Rep. 2011; 12:428–435. [PubMed: 21475249]

Van Allen EM, Wagle N, Sucker A, Treacy DJ, Johannessen CM, Goetz EM, Place CS, Taylor-Weiner A, Whittaker S, Kryukov GV, et al. The genetic landscape of clinical resistance to RAF inhibition in metastatic melanoma. Cancer Discovery. 2014; 4:94–109. [PubMed: 24265153]

Villanueva J, Vultur A, Lee JT, Somasundaram R, Fukunaga-Kalabis M, Cipolla AK, Wubbenhorst B, Xu X, Gimotty PA, Kee D, et al. Acquired Resistance to BRAF Inhibitors Mediated by a RAF Kinase Switch in Melanoma Can Be Overcome by Cotargeting MEK and IGF-1R/PI3K. Cancer Cell. 2010; 18:683–695. [PubMed: 21156289]

Vitari AC, Leong KG, Newton K, Yee C, O'Rourke K, Liu J, Phu L, Vij R, Ferrando R, Couto SS, et al. COP1 is a tumour suppressor that causes degradation of ETS transcription factors. Nature. 2011; 474:403–406. [PubMed: 21572435]

Wagle N, Emery C, Berger MF, Davis MJ, Sawyer A, Pochanard P, Kehoe SM, Johannessen CM, MacConaill LE, Hahn WC, et al. Dissecting therapeutic resistance to RAF inhibition in melanoma by tumor genomic profiling. Journal of Clinical Oncology. 2011; 29:3085–3096. [PubMed: 21383288]

Wagle N, Van Allen EM, Treacy DJ, Frederick DT, Cooper ZA, Taylor-Weiner A, Rosenberg M, Goetz EM, Sullivan RJ, Farlow DN, et al. MAP kinase pathway alterations in BRAF-mutant melanoma patients with acquired resistance to combined RAF/MEK inhibition. Cancer Discovery. 2014; 4:61–68. [PubMed: 24265154]

Wertz IE, O'Rourke KM, Zhang Z, Dornan D, Arnott D, Deshaies RJ, Dixit VM. Human De-etiolated-1 regulates c-Jun by assembling a CUL4A ubiquitin ligase. Science. 2004; 303:1371–1374. [PubMed: 14739464]

Whittaker SR, Theurillat JP, Van Allen E, Wagle N, Hsiao J, Cowley GS, Schadendorf D, Root DE, Garraway LA. A genome-scale RNA interference screen implicates NF1 loss in resistance to RAF inhibition. Cancer Discovery. 2013; 3:350–362. [PubMed: 23288408]

Yoon S, Seger R. The extracellular signal-regulated kinase: multiple substrates regulate diverse cellular functions. Growth Factors. 2006; 24:21–44. [PubMed: 16393692]

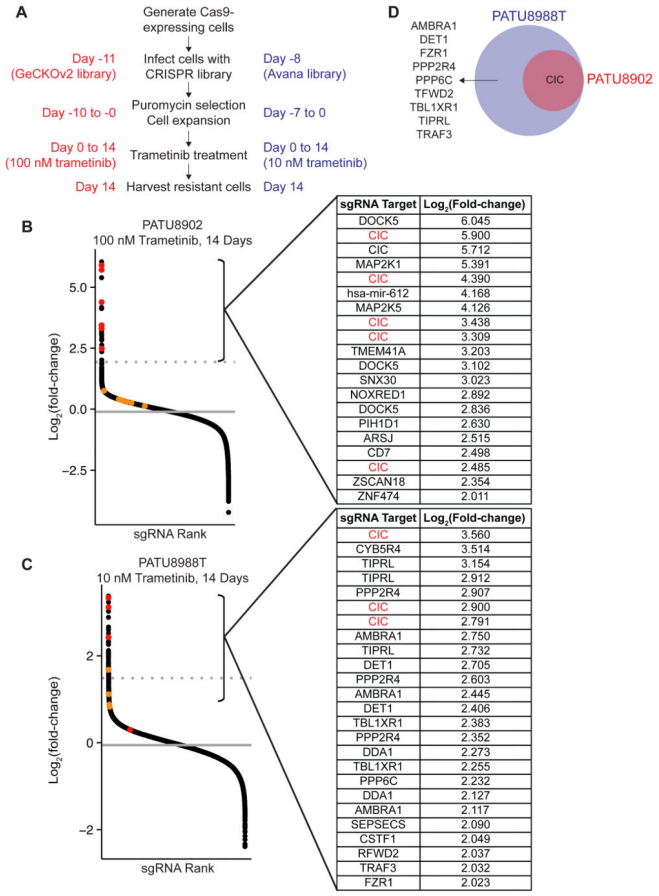

sgRNA Target	Log_2(Fold-change)
DOCK5	6.045
CIC	5.900
CIC	5.712
MAP2K1	5.391
CIC	4.390
hsa-mir-612	4.168
MAP2K5	4.126
CIC	3.438
CIC	3.309
TMEM41A	3.203
DOCK5	3.102
SNX30	3.023
NOXRED1	2.892
DOCK5	2.836
PIH1D1	2.630
ARSJ	2.515
CD7	2.498
CIC	2.485
ZSCAN18	2.354
ZNF474	2.011

sgRNA Target	Log_2(Fold-change)
CIC	3.560
CYB5R4	3.514
TIPRL	3.154
TIPRL	2.912
PPP2R4	2.907
CIC	2.900
CIC	2.791
AMBRA1	2.750
TIPRL	2.732
DET1	2.705
PPP2R4	2.603
AMBRA1	2.445
DET1	2.406
TBL1XR1	2.383
PPP2R4	2.352
DDA1	2.273
TBL1XR1	2.255
PPP6C	2.232
DDA1	2.127
AMBRA1	2.117
SEPSECS	2.090
CSTF1	2.049
RFWD2	2.037
TRAF3	2.032
FZR1	2.023

Figure 1. Genome Scale CRISPR-Cas9 Knockout Screens Identify Genes that Modulate Sensitivity to MEK Inhibition

(A) Outline of the pooled screening strategy.

(B, C) Distribution of log_2 fold-change in sgRNA representation on Day 14 versus the original sgRNA plasmid pool in PATU8902 cells treated with 100 nM trametinib (B) and in PATU8988T cells treated with 10 nM trametinib (C). Average of 2 biological replicates. Tables indicate all (B) or the 25 most (C) significantly enriched sgRNAs. Gray lines indicate average log_2 fold-change (solid) or 4 SD above average log_2 fold-change (dashed) of all screened sgRNAs. sgRNAs targeting *CIC* (red) and *ATXN1L* (orange) are indicated.

(D) Candidate mediators of resistance to trametinib identified from the PATU8902 and PATU8988T screens.

See also Figure S1 and Table S1.

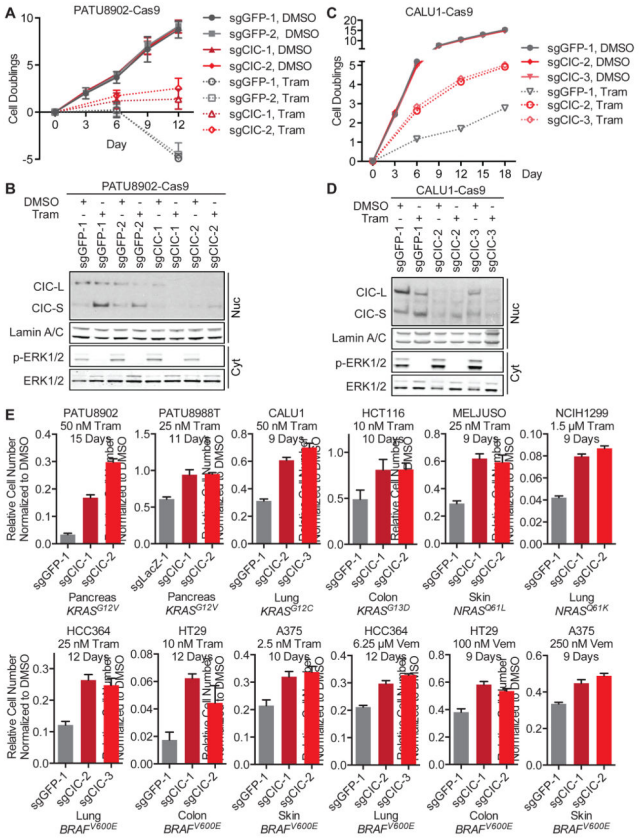

Figure 2. CIC Loss Modulates Sensitivity to MEK and BRAF Inhibition in Multiple Contexts

(A, C) Proliferation of PATU8902-Cas9 cells (A) or CALU1-Cas9 cells (C) expressing sgRNAs targeting *GFP* (control) or *CIC*, and treated with DMSO or 50 nM trametinib. 2 technical replicates of 2 independent experiments, data represented as mean ± SEM.

(B, D) Immunoblot analysis of expression levels of indicated proteins using PATU8902-Cas9 (B) or CALU1-Cas9 (D) fractionated cell lysates after 48 h of treatment with DMSO or 50 nM trametinib. Nuc = nuclear, Cyt = cytoplasmic.

(E) Long-term clonogenic proliferation assays to determine the effect of CIC^{KO} on trametinib (Tram) and vemurafenib (Vem) sensitivity in multiple lineage and mutation contexts. Cells were treated with the lowest concentration of inhibitor that robustly inhibited ERK phosphorylation (for MEK inhibitor) or MEK phosphorylation (for BRAF inhibitor) and induced proliferative arrest or cell death. 3 technical replicates representative of at least 2 independent experiments, data represented as mean ± SEM.

See also Figures S2 and S3.

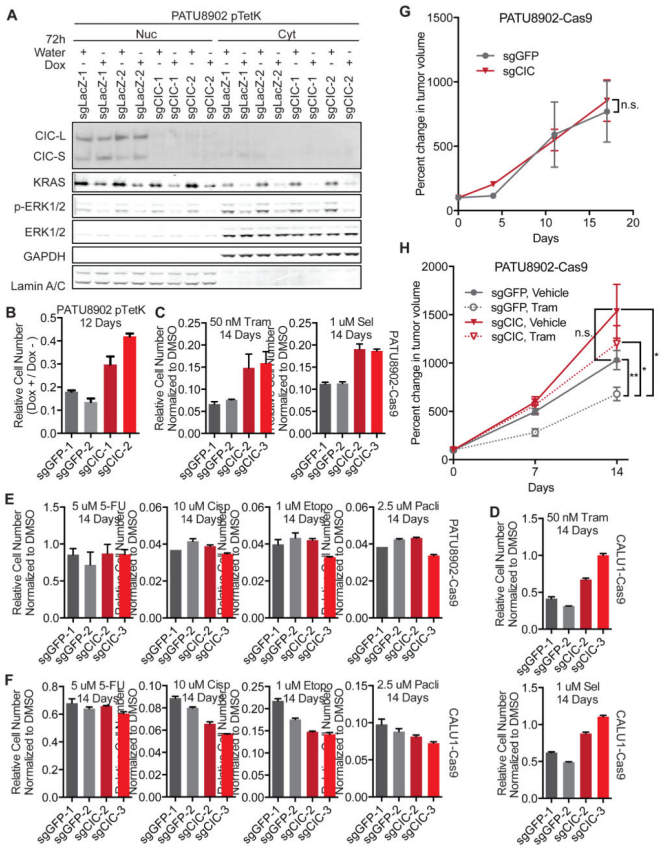

Figure 3. Reduced Drug Sensitivity Conferred by *CIC*^{KO} is Specific to RAS/MAPK Pathway and *CIC*^{KO} Modulates Sensitivity *In Vivo*

(A) Immunoblot assessment of KRAS depletion and phospho-ERK suppression in *CIC*^{WT} or *CIC*^{KO} PATU8902 pTetK cells treated with water or 1 μg/mL doxycycline (dox) for 72 h.

(B) Effect of *CIC*^{KO} on sensitivity to KRAS depletion in the KRAS-dependent cell line PATU8902 pTetK. Dox = doxycycline, 3 technical replicates representative of 2 independent experiments, data represented as mean ± SEM.

(C, D) Effect of *CIC*^{KO} on trametinib and selumetinib sensitivity in PATU8902-Cas9 (C) or CALU1-Cas9 (D) cells, 6 technical replicates representative of 2 independent experiments, data represented as mean ± SEM.

(E, F) Effect of *CIC*^{KO} on sensitivity to 5-FU, etoposide (etopo), or paclitaxel (pacli) in PATU8902-Cas9 (E) or CALU1-Cas9 (F). 3 technical replicates, data represented as mean ± SEM.

(G) Percent change in tumor volume of *CIC*^{WT} (sgGFP) or *CIC*^{KO} (sgCIC) PATU8902 xenografts in athymic nude mice. Average of 4 xenografts. Statistical significance determined by paired t-test, n.s = not statistically significant.

(H) Percent change in tumor volume of *CIC*^{WT} (sgGFP) or *CIC*^{KO} (sgCIC) PATU8902 xenografts in athymic nude mice receiving daily vehicle or trametinib treatment. Average of 10 xenografts, data are represented as mean ± SEM, tram = 2 mg/kg trametinib. Statistical significance determined using ANOVA and paired t-test. N.s. = not statistically significant, * = $p \leq 0.05$, ** = $p \leq 0.01$.

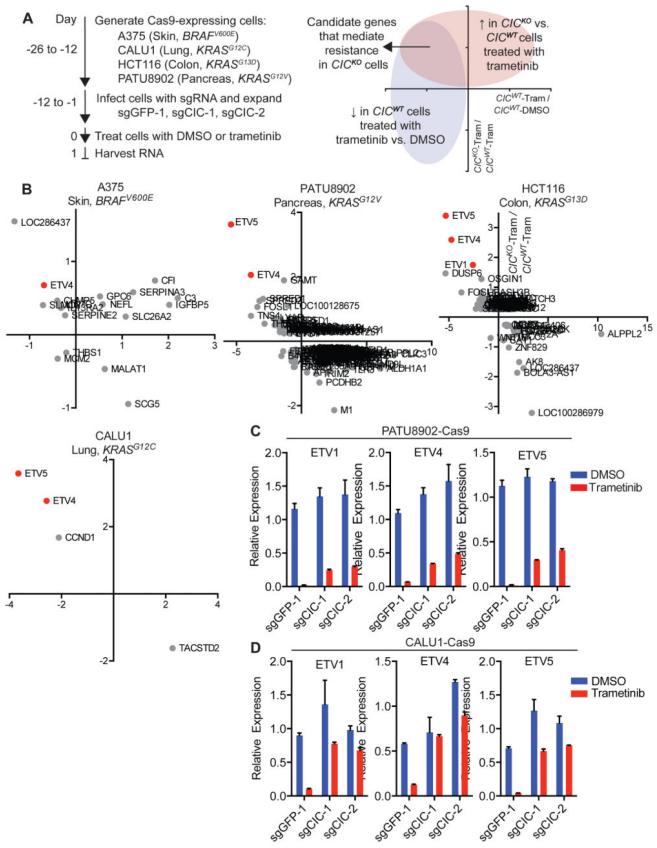

Figure 4. MEK Inhibition Increases Nuclear CIC-S and CIC-mediated Repression of ETS Transcription Factors

(A) Overview of RNA-sequencing strategy.

(B) Effect of trametinib treatment and *CIC*^{KO} on the transcriptome. Each point represents a gene that is significantly (q<0.05) differentially expressed between *CIC*^{KO} (sgCIC-1) and *CIC*^{WT} (sgGFP) cells treated with trametinib (*y*-axis), and between *CIC*^{WT} cells treated with trametinib versus DMSO (*x*-axis). Values represent average $\log_2$(fold-change) in expression of *2* technical replicates.

(C, D) qRT-PCR analysis of ETV1, 4, and 5 expression in *CIC*^{WT} or *CIC*^{KO} PATU8902 (C) or CALU1 (D) cells treated with DMSO or 50 nM trametinib for 24 h. Average of 3 independent experiments with 3 technical replicates, data represented as mean ± SEM.

See also Figures S4 and S5 and Table S2.

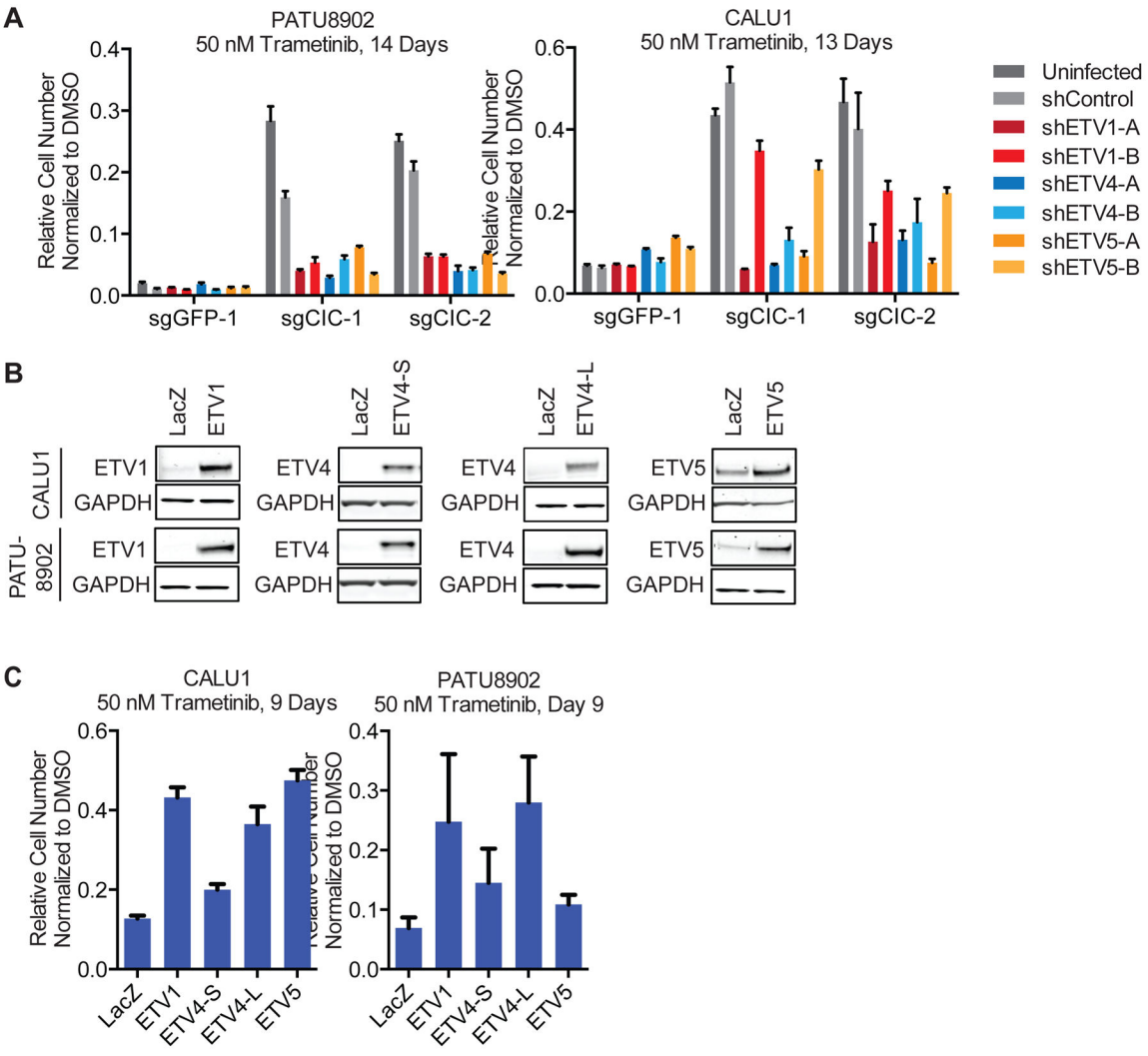

Figure 5. Increased Expression of ETV Transcription Factors is Necessary and Sufficient for Modulated Sensitivity to MEK Inhibition

(A) Long-term clonogenic proliferation assays to assess the effect of ETV1, 4, and 5 depletion on trametinib sensitivity in CIC^{WT} and CIC^{KO} cells. CIC^{WT} (sgGFP) and CIC^{KO} (sgCIC) PATU8902-Cas9 or CALU1-Cas9 cells expressing shRNAs targeting ETV1, ETV4, or ETV5 were treated with DMSO or trametinib. 3 technical replicates, representative of 2 independent experiments, data represented as mean ± SEM.

(B) Immunoblot analysis of CALU1or PATU8902 cells expressing the indicated ORFs.

(C) Long-term clonogenic proliferation assays to determine the effect of ETV1, ETV4-S, ETV4-L, or ETV5 overexpression on trametinib sensitivity in CALU1 or PATU8902 cells. 3 technical replicates, representative of 2 independent experiments, data represented as mean ± SEM.

See also Figure S6.

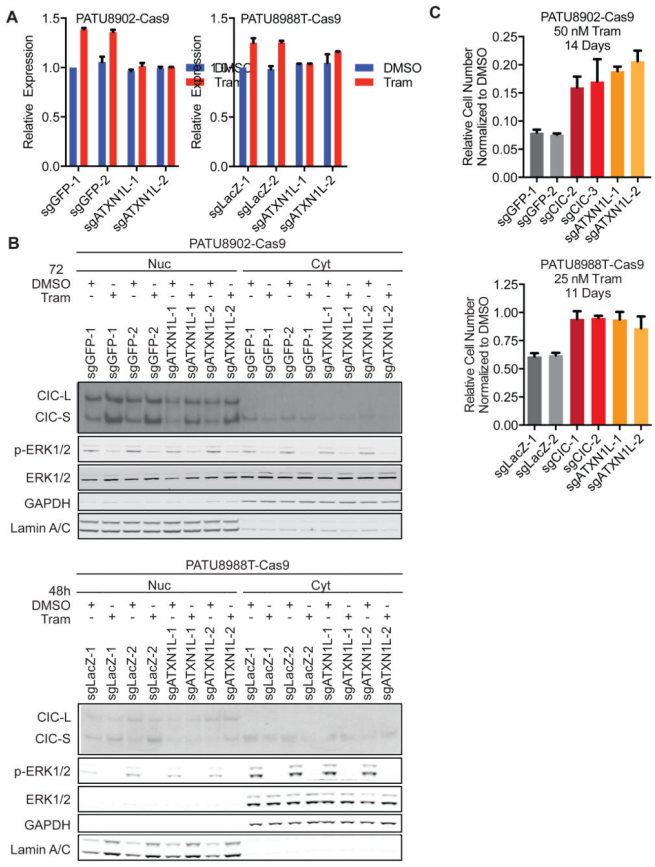

Figure 6. *ATXN1L* Deletion Modulates Trametinib Sensitivity by Reducing CIC Protein Levels

(A) qRT-PCR analysis of CIC expression in $ATXN1L^{WT}$ (sgLacZ) or $ATXN1L^{KO}$ (sgATXN1L) cells treated with DMSO or 50 nM trametinib for 24 h. Tram = trametinib, average of 3 independent experiments with 3 technical replicates, data represented as mean ± SEM.

(B) Immunoblot analysis of the effect of $ATXN1L^{KO}$ and trametinib treatment on CIC expression and localization using fractionated cell lysates after 48 h of drug treatment. Nuc = nuclear, cyt = cytoplasmic, tram = trametinib.

(C) Long-term clonogenic proliferation assay to determine the effect of $ATXN1L^{KO}$ on trametinib sensitivity. 3 technical replicates representative of 2 independent experiments, data represented as mean ± SEM.

See also Figure S7

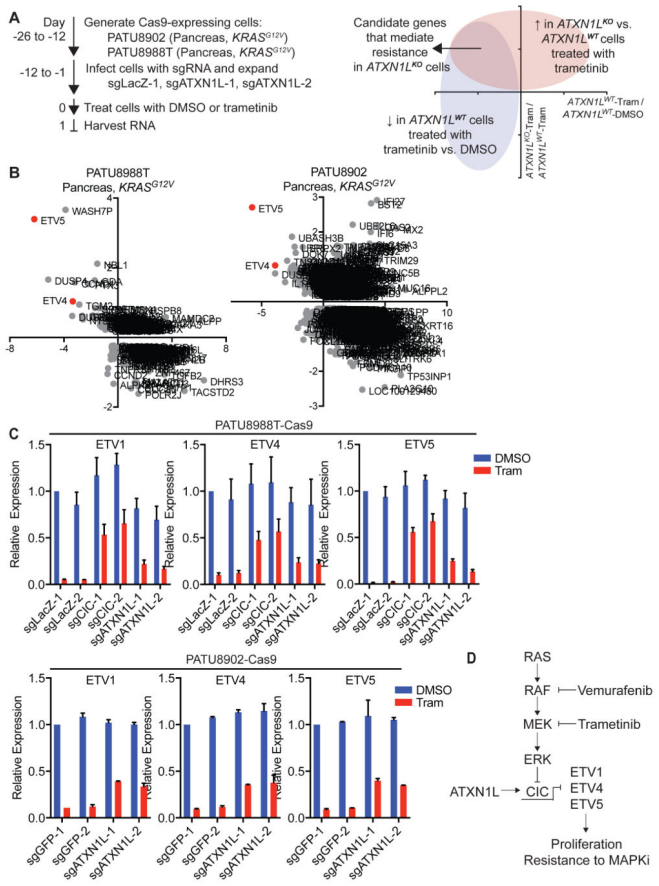

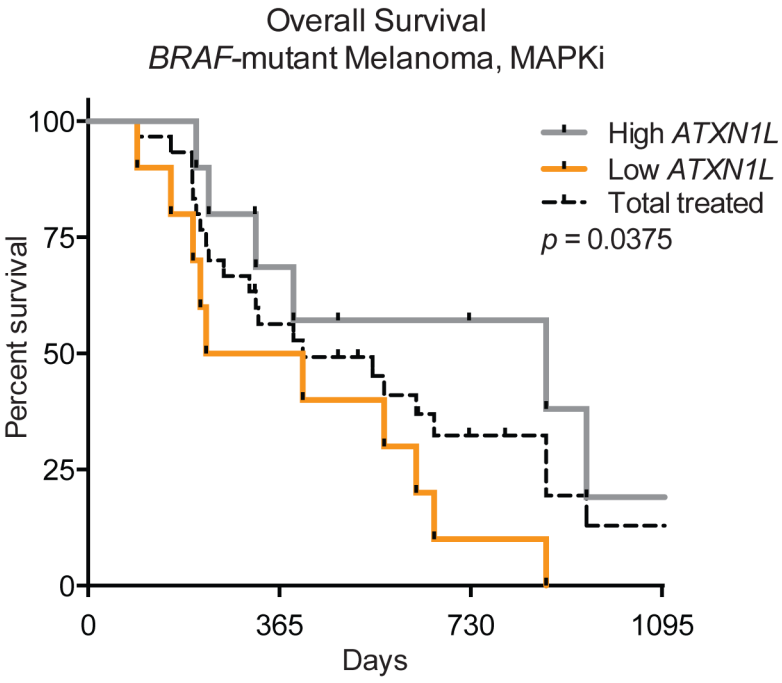

Figure 7. *ATXN1L* Deletion Modulates Trametinib Sensitivity by Increasing Expression of ETS Transcription Factors

(A) Overview of RNA-sequencing strategy.

(B) Effect of trametinib treatment and $ATXN1L^{KO}$ on the transcriptome. Each point represents a gene that is significantly ($q<0.05$) differentially expressed between $ATXN1L^{KO}$ (sgATXN1L-2) and $ATXN1L^{WT}$ (sgLacZ) cells treated with trametinib (*y*-axis), and between $ATXN1L^{WT}$ cells treated with trametinib versus DMSO (*x*-axis). Values represent average $\log_2$(fold-change) in expression of 2 technical replicates.

(C) qRT-PCR of ETV1, 4, and 5 expression in PATU8988T or PATU8902 control (sgLacZ), CIC^{KO} (sgCIC), or $ATXN1L^{KO}$ (sgATXN1L) cells treated with DMSO or 50 nM trametinib for 24 h. Tram = trametinib, average of *2* independent experiments, data are represented as mean ± SEM.

(D) Proposed mechanism of trametinib and vemurafenib resistance mediated by CIC or ATXN1L loss. MAPKi = MAPK pathway inhibition.

(E) Kaplan-Meier curve depicting overall survival of 30 patients with *BRAF*-mutant melanoma who received MAPK pathway inhibitor therapy. 'High *ATXN1L*' and 'Low *ATXN1L'* groups include the 10 patients with highest or lowest pre-treatment *ATXN1L* expression, respectively.

See also Figure S7 and Table S3.